



High performance concretes at elevated temperature : permeability and microstructure

Tsimbrovska M.⁽¹⁾, Kalifa P.⁽¹⁾, Quenard D.⁽¹⁾, Daïan J.F.⁽²⁾

(1) CSTB, France

(2) LTHE/IMG, France

ABSTRACT

Due to their low porosity high performance concretes are subject to spalling when exposed to elevated temperature. The key parameter in spalling is permeability. In this work the evolution of permeability and microstructure with temperature (up to 400°C) is studied. The important increase in permeability (2 orders of magnitude) is correlated to evolution of fine porosity due to dehydration up to 300°C, then to cracking that appeared between 300 and 400°C.

INTRODUCTION

Due to their high compactness and their low permeability, high performance concretes (HPC) are used more and more in construction (high rise buildings, tunnels, bridges, nuclear power plants). However, when they are subjected to high temperatures, such as during a fire or a nuclear accident, these compact concretes, unlike ordinary concretes, may behave in a brittle way. Sometimes we observe several centimetre thick concrete pieces scaling off. This is important enough for Eurocode-2 to have reservations about the use of HPCs. This spalling phenomenon was found on high performance concrete and mortar specimens, heated up to 250-400°C, even at slow temperature rates (1°C/min) [1-2].

One of the key parameters governing spalling is the material permeability which controls fluid transfers. The main process at the origin of spalling is the establishment of high pressure gradients in the porous network. As concrete heats up, there is an evaporation of the water contained in the pores and the water freed following the dehydration reaction (beginning at 180°C). The lower the permeability, the higher the pressure. Furthermore, the knowledge of concrete permeability is primordial to ensure the tightness of nuclear reactor vessels.

In spite of its importance, the permeability of HPC brought to high temperatures has not been widely studied. It was reported that when concretes are heated, their permeability increases because of the reduction in water content [3-4]. However, the permeability of porous materials is not only defined by its water content but also by its microstructure, that is, porosity, connectivity, pore size distribution and cracking. The study of the microstructure of HPCs and ordinary concretes heated up to 600°C, shows a considerable increase in the total porosity and in pore dimension [5-7]. The evolution of the microstructure was observed using a Scanning Electron Microscope (SEM) on fractures of HPCs. A homogeneous degradation of the structure of this material was found at 400°C [8], probably due to the dehydration reaction, and cracks appeared at 600°C [9].

In the present work, an analysis was made of the evolution with temperature (up to 400°C) of the intrinsic permeability of a high performance mortar in correlation with its microstructure. The latter is characterised by total porosity, pore size distribution, density and opening of the cracks observed with an optical microscope and a SEM.

SPECIMEN MANUFACTURING AND CONDITIONING

Our study was carried out on two mortars: a high performance mortar (HPM) and an ordinary mortar (OM). 24 hours after the specimens (plates 160x120x40 mm³) were made, they were demolded and placed in sealed bags for 90 days. The nominal compressive strength was measured on specimens (40 mm)³ after being cured in water for 28 days. The composition of both mortars, as well as their compressive strength are shown in Table 1.

	HPM	OM
	Weight, g	Weight, g
Calcareous sand 0/5 (Boulonnais)	633.6	-
Silico-calcareous sand 0/5 (Seine)	633.6	-
siliceous sand 0/2	-	1467.4
Cement	818.4	488.4
Microsilica (S)	81.6	
Admixture	14.4	
Water	218.4	244.2
w/(c+S)	0.24	0.5
R _c , MPa	105.4	69,5

Table 1. Composition and compressive strength of HPM and OM

THERMAL TREATMENT

We measured the residual properties of heated materials that is after they were cooled down to room temperature. The properties of the material brought to high temperatures are compared with those of the material dried at 105°C. All thermal treatments, including drying, were carried out until the steady mass state was reached, in order to ensure the same water content, which we define as the dry state. The material was brought to the target temperature (105, 200, 300 and 400°C) in a ventilated electric oven at a rate of 0.2°C/min. The temperature then remained constant for several hours (several days in the case of drying at 105°C) until the specimen reached weight stability. The specimens were cooled in the oven at the same rate of 0.2°C/min. This low heating and cooling rate is meant to avoid internal stresses due to thermal gradient. After heating, the specimens were kept in sealed bags containing silica gel to prevent the material from re-humidifying.

MEASUREMENTS OF PARAMETERS

The permeability measurements were performed on cylinders of 54 mm diameter and 30 mm thickness, drilled from the mortar plates. Each permeability value is the average obtained on a

minimum of 3 specimens. The variable pressure permeameter developed at I.N.S.A. of Toulouse (France) was used (Fig.1). It is described in [10]. The coefficient of permeability is calculated according to Darcy's Law, for a laminar steady state flow through a porous medium. The complete theory, taking the air compressibility into account is used [10]:

$$k = \frac{\mu s L}{\rho_l A g t} \left[(1 + \epsilon) \ln \frac{h_0}{h} - \frac{(3 - \epsilon)(h_0 - h)}{2H} \right] \quad (1)$$

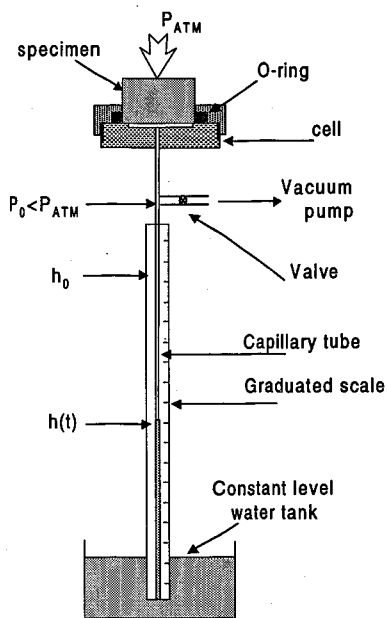


Figure 1. Permeameter diagram

where :

$$\epsilon = \left(h_0 + \frac{V_0}{s} \right) \frac{1}{H} ; \text{ and}$$

k - Coefficient of intrinsic permeability;

μ - Atmospheric air viscosity;

s - Tube section;

L - Specimen height;

A - Specimen section;

ρ_l - Specific weight of the pressure gauge liquid (water);

g - Gravity acceleration;

h_0 - Initial water level;

h - Water level at time t;

V_0 - Volume of air contained between the base of the specimen, the valve and the initial water level.

The total volume porosity was measured on cubes 40 mm per side, by water saturation under vacuum. The experimental procedure is inspired by ISO Standard 5017: 1988. Each porosity value is the average obtained on a minimum of 3 specimens.

The pore size distribution was obtained using mercury intrusion porosimetry (MIP). The measurements were carried out on HPM cubes, 10 mm per side. With this method, pores ranging between 10 and 0.004 μm were investigated. The diameter of pores D is calculated by using Laplace's Law and a model of cylindrical pores of equivalent diameter:

$$D = \frac{4\sigma \cos \theta}{p} \quad (2)$$

where p is the corresponding mercury pressure, σ is the surface tension of the mercury and θ is the contact angle for the mercury-air-concrete interface.

The damage of material was quantified using an optical microscope and a SEM, coupled with an image analysis system. These observations require a surface preparation by polishing. However, in a previous work, we found that, in the case of heated concretes, the polishing modifies the structure [8]. Actually, because of the dehydration, the material's structure becomes crumbly and the polishing degrades the surface. To maintain the integrity of the structure, the material was impregnated with epoxy resin under vacuum. The use of a

fluorescent agent added to the resin, made it possible to highlight the cracks (Fig.5). Before their characterisation, the specimens ($18 \times 18 \times 10 \text{ mm}^3$) were polished down to $3 \mu\text{m}$.

The crack images, taken with the fluorescent optical microscope, were thresholded by image processing. The crack specific surface defined as the length of crack per unit surface area was calculated by using the intercepts method [11]. The crack opening was estimated on SEM images (Fig.6).

RESULTS AND DISCUSSION

After drying at 105°C , HPM has a permeability one order of magnitude smaller than that of OM (Fig.2). The permeability of HPM increases rapidly with temperature and at 400°C , it gains 2 orders of magnitude. On the other hand the development of this property is less pronounced in OM: at 400°C , the permeability increases by 1 order of magnitude. One notes the small standard deviations on the measurements. The values of permeability and porosity are reported in Table 2.

Temperature, $^\circ\text{C}$	Total porosity, %		Permeability, 10^{-16} m^2	
	MO	MHP	MO	MHP
105	16.66 ± 0.06	14.27 ± 0.46	0.99 ± 0.05	0.16 ± 0.02
200	18.36 ± 0.07	16.27 ± 0.54	1.22 ± 0.03	0.76 ± 0.03
300	18.04 ± 0.08	17.00 ± 0.14	3.23 ± 0.26	3.40 ± 0.25
400	19.65 ± 0.50	17.29 ± 0.21	8.15 ± 1.22	15.5 ± 1.92

Table 2. Evolution of permeability and porosity with temperature

The water porosity measurements show that at 105°C , HPM is more compact than OM (Fig.3). We observe an overall increase in the porosity up to 400°C for both materials. However, MO shows a slight decrease in porosity between 200 and 300°C . Since the data dispersion is low enough, this tendency is attributed to an actual changes in the microstructure. Similar results were obtained by Piasta et al [5] in the case of a cement paste ($w/c=0.4$). The drop in the total porosity of the OM at 300°C is probably due to the re-crystallisation of amorphous $\text{Ca}(\text{OH})_2$ and also to the additional hydration of the anhydrous which takes place at 300°C under the so-called internal autoclaving conditions [5]. Piasta et al [5], with the aid of X-ray diffraction, noted a considerable increase in the $\text{Ca}(\text{OH})_2$ in the hardened cement paste ($w/c=0.4$) heated up to 300°C . This densification phenomenon is less pronounced in the case of HPM because the quantity of $\text{Ca}(\text{OH})_2$ is smaller in concretes containing microsilica. This is because the portlandite is consumed by the silica as part of the pozzolanic reaction, to form CSHs. The drop in the quantity of $\text{Ca}(\text{OH})_2$ in concretes containing microsilica was noted with the aid of X-ray diffraction [9] and by differential thermal analyses [7]. However as Figures 3 and 4 show, this densification appears for the capillary porosity of HPM measured by MIP.

In the case of the OM, this development of total porosity has no direct influence on permeability. Even though the porosity diminishes from 200 to 300°C , the permeability still increases. This permeability evolution is probably due to the increase in a class of pores, which modifies the connectivity of the network.

The MIP applied to HPM gives total porosity values which are about 2 times less than those measured by water saturation (Fig.3). This points out a large volume of pores with

diameters less than 4 nm (the same size as the CSH gel pores), which are not accessible by this method. So we found that the evolution of the total porosity of HPM up to 300°C is essentially due to the increase in the volume of these fine pores, caused by the dehydration which takes place from 180 to 300°C. This is because the volume of capillary pores, accessible by MIP, does not evolve at 200°C and diminishes slightly at 300°C (Fig.3-4). The evolution of the fine pores probably causes an increase in the network connectivity which, in turn, causes a

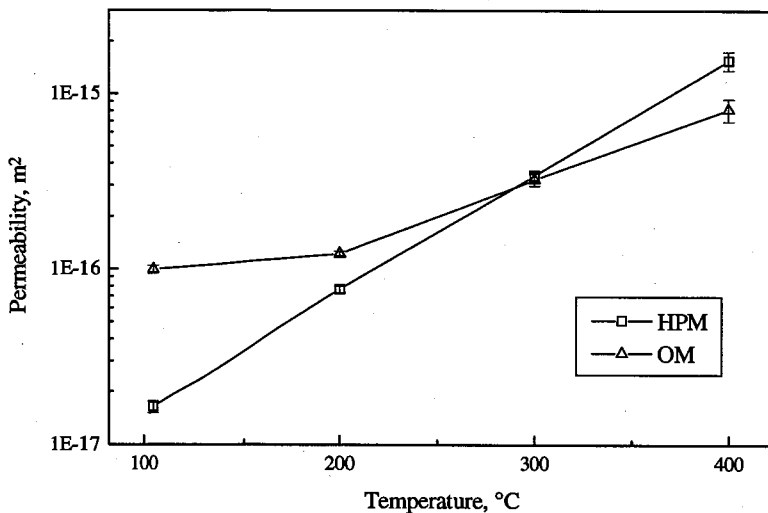


Figure 2. Permeability versus temperature.

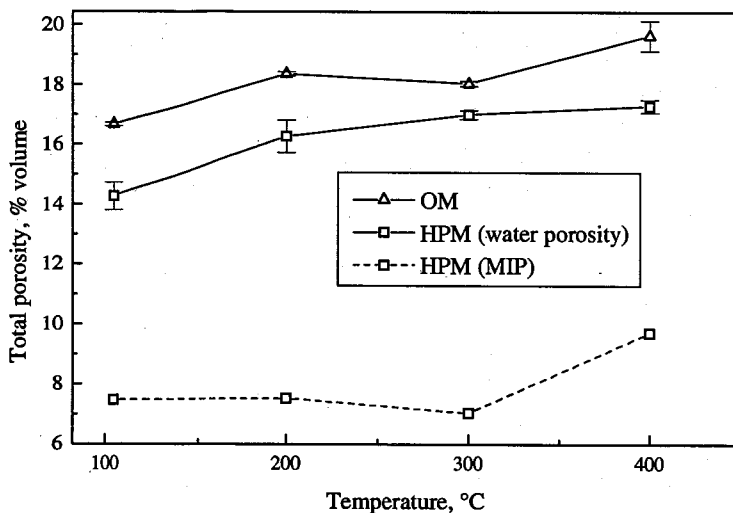


Figure 3. Total porosity versus temperature

rapid evolution of permeability. So we find that in the case of HPM, the evolution of the permeability with temperature (up to 300°C) is not due to the evolution of the capillary porosity, but to the evolution of the fine porosity.

The differential distribution curve of HPM pore diameters, dried at 105°C, indicates a large population of capillary pores with diameter 30 nm (first peak) and another group of larger pores, with diameter 400 nm (second peak) (Fig.4). At 200°C, there is not much evolution in the diameter of the pores. The first peak diminishes at 300°C and increases again at 400°C.

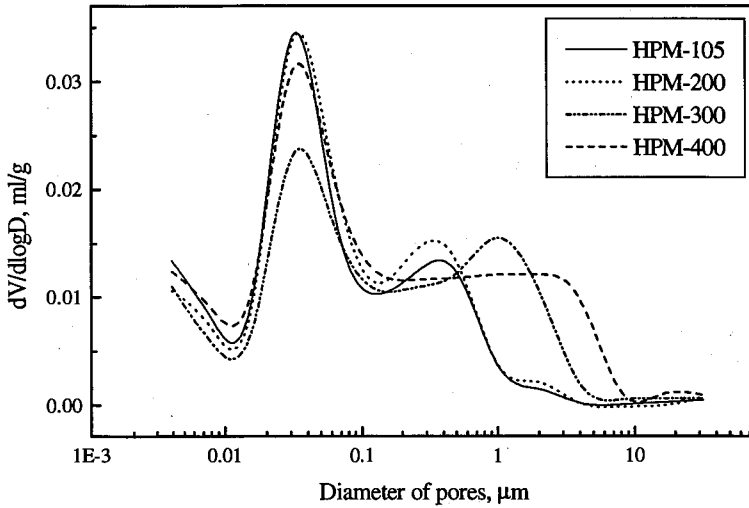


Figure 4. Distribution of pore diameters in HPM.

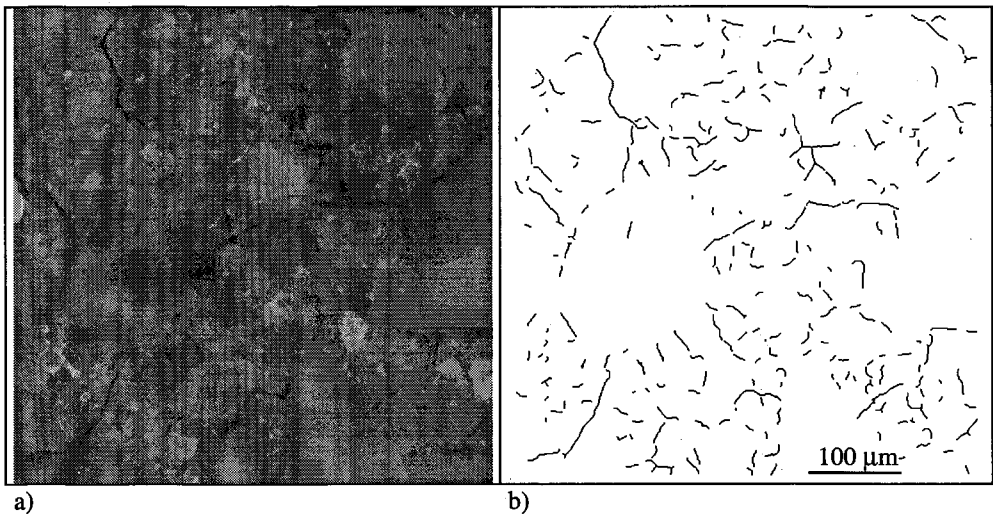


Figure 5. Network of cracks in HPM, heated to 400°C:
a) observed through optical microscope; b) thresholded by image processing.

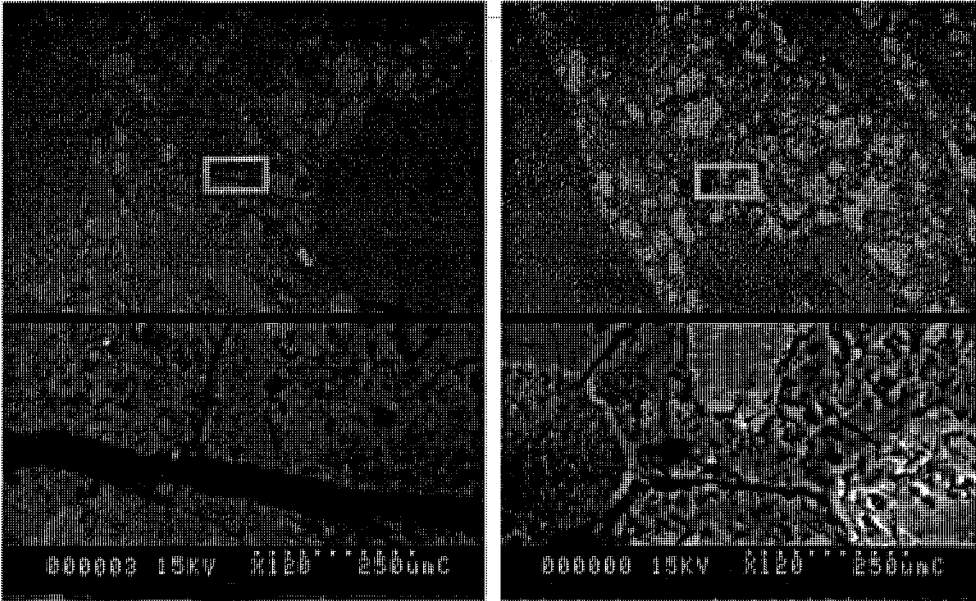


Figure 6. Cracking of HPM, heated to 400°C, observed through SEM.

At 300°C, the second peak shifts toward the larger pores and at 400°C this zone becomes more spread out. We also find an increase in the quantity of pores less than 6-7 nm. This assumes a large volume of fine pores (of the size of the CSH gel pores) and confirms the result obtained by the porosity measurements.

The observation of microstructure has shown that no visible cracking appears in the OM. On the other hand, in HPM, from 300 to 400°C, we observe a homogeneous cracking of the matrix (Fig.5-6). The cracks link and bypass the sand grains. The average specific surface of the cracks, calculated by image analysis, is $0.02 \mu\text{m}^{-1}$ (Fig.5b) and their opening varies from a few tenths of a micron to 5-7 microns (Fig.6). On the pore diameter distribution curve, the appearance of cracks is indicated by a flattened curve zone (Fig.4) from 0.1 to 5 μm . This size corresponds to the opening of the cracks.

The appearance of the network of cracks in HPM from 300° to 400°C explains the rapid evolution of permeability at those temperatures (Fig.2).

CONCLUSIONS AND PROSPECTIVES

The purpose of this work was to study the effect of temperature on permeability and on the microstructural characteristics of HPM. This provided us with the following results.

The evolution with temperature of the intrinsic permeability of HPM is greater than for the OM. After the drying at 105°C, although HPM has a lower permeability than OM, at 400°C, the reverse is true.

Up to 300°C, this substantial evolution of HPM permeability is due to the increase in the volume of fine pores, following cement paste dehydration, and is not at all influenced by the evolution of capillary porosity.

The case of OM makes it possible to point out that the total porosity cannot be considered as the only parameter controlling permeability. Each category of pores may be responsible for a change in connectivity, and therefore in permeability. In the present study, we found out in HPM an increase of connectivity in gel pore size porosity up to 300°C, and in capillary size porosity due to cracking at 400°C.

The application of the resin impregnation technique allowed to highlight that severe cracking appears in HPM from 300°C. The opening of the cracks varies from 0.1 to 7 µm. This cracking is certainly responsible for the striking increase in permeability at those temperatures.

This experimental work constitutes the first step in our study. A model linking permeability to microstructure and, in particular, to cracking is currently being developed.

ACKNOWLEDGEMENTS

We thank Mr. C. Gauthier of the LCPC (France) and Mr. D. Giraud of the CSTB for their contribution to this study.

REFERENCES

1. Hertz, K. 1984. Heat-induced explosion of dense concretes. *Technical University of Denmark, Institute of Building Design Report N° 166.*
2. Noumowe, A., P. Clastres, G. Debicki, M. Bolvin 1994. Effect of high temperature on high performance concrete (70-600°C) - Strength and porosity. *Third CANMET/ACI International Conference on Durability of concrete: 157-172.*
3. Maréchal, J.C., M. Beaudoux 1992. Transfert diphasique expérimental sur une paroi épaisse de béton soumise à une élévation rapide de pression et de température. *Annales de l'Institut technique du bâtiment et des travaux publics: 74-111.*
4. Ujike, I., R. Sato, S. Nagataki 1995. A study on air permeability of concrete under elevated temperatures. *Concrete Under Severe Conditions: Environment and loading :443-452.*
5. Piasta, J., Z. Sawicz, L. Rudzinski 1984. Changes in the structure of hardened paste due to high temperature *Materials and Structures 100: 291-296.*
6. Jumppanen, U-M., U. Diederichs, K. Hinrichsmeyer 1986. Material properties of F-concrete at high temperatures. *Espoo : Technical Research Centre of Finland 542: 60.*
7. Diederichs U., U-M. Jumppanen, V. Penttala 1989. Behaviour of high strength concrete at high temperatures. *Espoo : Helsinki University of Technology Report 92: 15-26.*
8. Tsimbrovska, M. 1994. Comportement des Bétons à hautes performances aux températures élevées, état des lieux et approche de la dégradation microstructurale. *Rapport du DEA INPG-CSTB.*
9. Saad, M., S.A. Albo-El-Einein, G.B. Hanna, M.F. Kotkata 1996. Effect of silica fume on the phase composition and microstructure of thermally treated concrete. *Cement and Concrete Research 26(8): 1479-1484.*
10. Yssorche, M.P., J.P. Bigas, J.P. Ollivier 1995 Mesure de la perméabilité à l'air des bétons au moyen d'un perméamètre à charge variable. *Materials and Structures 28(181): 401-405.*
11. Stroeven, P. 1979. Geometric probability approach to the examination of microcracking in plain concrete. *Journal of Material Science 14: 1141-1151.*